Original article

Nuclear Medicine Communications

^{18}F-FCho PET and MRI for the prediction of response in glioblastoma patients according to the RANO criteria

Julie Bolcaen[a], Marjan Acou[b], Tom Boterberg[c], Christian Vanhove[e], Filip De Vos[f], Caroline Van den Broecke[d], Roel Van Holen[e], Karel Deblaere[b] and Ingeborg Goethals[a]

Purpose **In this study, we investigated fluorine-18 fluoromethylcholine (^{18}F-FCho) PET and contrast-enhanced MRI for predicting therapy response in glioblastoma (GB) patients according to the Response Assessment in Neuro-Oncology criteria. Our second aim was to investigate which imaging modality enabled prediction of treatment response first.**

Materials and methods **Eleven GB patients who underwent no surgery or debulking only and received concomitant radiation therapy (RT) and temozolomide were included. The gold standard Response Assessment in Neuro-Oncology criteria were applied 6 months after RT to define responders and nonresponders. ^{18}F-FCho PET and MRI were performed before RT, during RT (week 2, 4, and 6), and 1 month after RT. The contrast-enhancing tumor volume on T1-weighted MRI (GdTV) and the metabolic tumor volume (MTV) were calculated. GdTV, standardized uptake value $(SUV)_{mean}$, SUV_{max}, MTV, $MTV \times SUV_{mean}$, and percentage change of these variables between all time-points were assessed to differentiate responders from nonresponders.**

Results **Absolute SUV values did not predict response. MTV must be taken into account. ^{18}F-FCho PET could predict response with a 100% sensitivity and specificity using $MTV \times SUV_{mean}$ 1 month after RT. A decrease in GdTV between week 2 and 6, week 4 and 6 during RT and week 2 during RT, and 1 month after RT of at least 31%, at least 18%, and at least 53% predicted response with a sensitivity and specificity of 100%. As such, the parameter that predicts therapy response first is MR derived, namely, GdTV.**

Conclusion **Our data indicate that both ^{18}F-FCho PET and contrast-enhanced T1-weighted MRI can predict response early in GB patients treated with RT and temozolomide.** ***Nucl Med Commun*** **38:242–249**

Nuclear Medicine Communications 2017, **38**:242–249

Keywords: fluorine-18 fluoromethylcholine, glioblastoma, MRI, PET, therapy response

Departments of [a]Nuclear Medicine, [b]Radiology, [c]Radiation Oncology, [d]Pathology, Ghent University Hospital, [e]MEDISIP, Department of Electronics and Information Systems, iMinds Medical IT and [f]Department of Radiopharmacy, Ghent University, Ghent, Belgium

Correspondence to Julie Bolcaen, MSc, Ghent University Hospital, Nuclear Medicine 0P8, De Pintelaan 185, 9000 Ghent, Belgium
Tel: +32 332 30 28; fax: +32 332 38 07; e-mail: julie.bolcaen@ugent.be

Received 17 June 2016 **Revised** 12 August 2016 **Accepted** 16 August 2016

Introduction

Glioblastoma (GB) is the most malignant and most common glioma type in adults, accounting for 60–70% of all malignant gliomas, and has a high morbidity and mortality rate [1]. For newly diagnosed patients with a good performance status, the standard of care includes maximal surgical resection, followed by combined external beam radiation therapy (RT; 60 Gy in 30 fractions) and temozolomide (TMZ; 75 mg/m^2 for 6 weeks), and maintenance TMZ (150–200 mg/m^2/day × 5 days, every 28 days for six cycles) [2–4]. Even with optimal treatment, the median survival is only 12–15 months [1]. Several prognostic factors have been identified in patients with GB, such as age, Karnofsky performance status, neurological status, WHO tumor grade, tumor location, extent of surgery, genetic and molecular biomarker status, and concomitant TMZ [5,6].

Until 2010, mainly MacDonald criteria were used for assessing response to therapy in high-grade glioma. The criteria are based on two-dimensional tumor measurements on computed tomography (CT) or MRI, in addition to a clinical assessment and corticosteroid use and dose [7]. However, in 20–30% of patients, pathological contrast enhancement subsiding without any change in therapy is shown on the first postirradiation MRI. This phenomenon, known as pseudoprogression, likely results from transiently increased permeability of the tumor vasculature from irradiation and complicates the determination of tumor progression immediately after the completion of radiotherapy. In addition, it is worth mentioning that pseudoprogression is more frequently encountered since the introduction of TMZ in the treatment protocol for GB [1,7]. In an attempt to more accurately assess treatment response, new response criteria for Response Assessment in Neuro-Oncology (RANO) were introduced in 2010, including the tumor size (in two-dimensional) as measured on T2-weighted and Fluid Attenuated Inversion Recovery (FLAIR) – weighted

DOI: 10.1097/MNM.0000000000000638

images in addition to the contrast-enhancing tumor part [7]. However, increased enhancement after the administration of gadolinium and FLAIR/T2 hyperintense signal abnormalities can also occur because of treatment-related inflammation, postsurgical changes, subacute irradiation effects, and radiation necrosis [7,8]. As is the case for the MacDonald criteria, the RANO criteria also do not take into account changes in tumor biology, which may precede anatomical changes of the tumor volume [1,9]. To visualize changes in tumor biology, functional imaging techniques assessing for example proliferative activity or hypoxia are needed [10]. Fluorine-18 fluorodeoxyglucose (^{18}F-FDG) PET, estimating glucose metabolism of (tumor) cells, enables monitoring therapeutic response in brain tumors with a greater specificity than CT or MRI [1]. However, a major disadvantage of ^{18}F-FDG is its high uptake in normal brain tissue, decreasing the sensitivity of ^{18}F-FDG PET for detecting recurrent or residual glioma [1]. Delayed ^{18}F-FDG PET imaging may, however, overcome this problem [1,11]. Our group showed that ^{18}F-FDG PET imaging at a delayed interval (300 min injection) better distinguishes tumor from normal gray matter than imaging at conventional intervals (60 min after injection). Spence *et al.* [12] performed kinetic modeling and found that this was because of a faster tracer clearance from normal brain tissue than from tumor [1,11,12]. Fluorine-18 fluoroethyltyrosine (^{18}F-FET) PET is also a promising tool for treatment monitoring of brain tumors [13–15], with ^{18}F-FET being able to detect tumor progression earlier than MRI [8]. Also, ^{18}F-FDOPA PET identified treatment responders (R) to antiangiogenic therapy as early as 2 weeks after treatment initiation [16]. In the present study, we investigated fluorine-18 fluoromethylcholine (^{18}F-FCho) PET and MRI for response prediction in a homogeneous population of GB patients treated with the Stupp regimen [3]. In our study, we performed PET and MRI scans before the start of treatment (before RT), during RT (2, 4, and 6 weeks), and 1 month after the completion of RT (after RT). Our first aim was to investigate whether therapy response can be predicted by ^{18}F-FCho PET and MRI. Second, we investigated which imaging modality enables prediction of therapy response first.

Materials and methods

Patients and treatments

A homogeneous population of 11 GB patients was included in this study. There were three women and eight men. Inclusion criteria were as follows: (a) histopathologically proven GB, (b) no surgery or debulking/submaximal resection only, and (c) treatment with conformal external beam RT (60 Gy in 30 fractions) and TMZ (75 mg/m^2 for 6 weeks). The study was approved by the local ethics committee and all patients provided written informed consent. Detailed patient characteristics are shown in Table 1.

Response assessment

Taking into account a median survival of 12–15 months in GB patients receiving optimal treatment, RANO criteria were applied arbitrarily 6 months after the completion of RT to divide the patients into two categories: R [including partial responder (PR) and complete responder (CR)] and nonresponders [NR, including stable disease (SD) and progressive disease (PD)] (Tables 1 and 2) [7].

PET imaging with ^{18}F-FCho

^{18}F-FCho PET scans were acquired before the start of concomitant RT and TMZ treatment (before RT), during RT (at weeks 2, 4, 6), and 1 month after RT. Missing data are shown in Table 1. The brain PET scans were acquired using a PET Allegro system (Philips Healthcare, Cleveland, Ohio, USA), which consists of a gadolinium oxyorthosilicate full-ring PET scanner with a spatial resolution of 5.0 mm (full-width at half-maximum). The system can acquire the whole brain using one bed position [field of view (FOV), Z-axis = 18 cm]. PET images were acquired with a voxel size of $2 \times 2 \times 2$ mm in a matrix of 128×128. The PET system also includes cesium sources for transmission scanning. The patients had fasted for at least 6 h before ^{18}F-FCho was administered to avoid competition effects on ^{18}F-FCho transport across the cell membrane. A transmission scan of the head was performed first. Subsequently, the patients received an intravenous injection of 296–370 MBq (8–10 mCi) of ^{18}F-FCho that was synthesized using the method of Slaets *et al.* [17]. The PET images were reconstructed using a three-dimensional (3D) row action maximum likelihood algorithm provided by the manufacturer. Attenuation and scatter correction were applied. A 5-min image acquired 25–30 min after injection was used for the analysis.

Semiquantitative PET analysis

Standardized uptake values (SUVs) were calculated using PMOD software (version 3.405; PMOD Technologies, Zürich, Switzerland). The SUV reflects the ratio of the decay-corrected activity in tissue per milliliter and the injected activity per patient body weight. In PMOD, the metabolic tumor volume (MTV) was defined using an automatic method applying a fixed threshold of 40% of the maximum SUV value (SUV_{max}) [18]. The 40% threshold was used because it corresponded best to the visually metabolically active tumor on the ^{18}F-FCho PET images. In addition, because it only makes sense to investigate treatment response (because of RT) within the tissue volume that received irradiation, the 40% threshold was applied within the 95% isodose of the RT plan (Fig. 1). The 95% isodose reflects the volume that received at least 95% of the prescribed irradiation dose. It is worth mentioning that none of the patients showed increased ^{18}F-FCho uptake beyond the 95% isodose. Thus, first, ^{18}F-FCho PET and planning CT scans were

Table 1 Patient characteristics

Patients number	Sex	Age (years)	Surgery	Tumor location	Multifocal disease	Concomittant radiation and chemotherapy	Pretreatment MTV (40% SUV_{max}) (ml)	PET and MRI acquisition[a]					Response assessment 6 months post-RT[b]
								Pre-RT	W2	W4	W6	M1	
1	Male	49	Biopsy	Temporal lobe	–	60 Gy 145 mg/day	4.8	✓	✓	✓	✓	✓	PD
2	Female	47	Biopsy	Temporal lobe	–	60 Gy 150 mg/day	37.8	✓	✓	✓	✓	✓	PR
3	Male	41	Biopsy	Parietal lobe	+	60 Gy 150 mg/day	18.3	✓	✓	✓	✓	✓	PD
4	Male	65	Biopsy	Frontal lobe	+	60 Gy 135 mg/day	5.3	✓	✓	✓	✓	✓	PD
5	Male	61	Debulking only	Frontal and temporal lobe	–	60 Gy 150 mg/day	3.9	✓	✓	✓	✓	✓	PR
6	Female	49	Biopsy	Temporal lobe	–	60 Gy 125 mg/day	5.5	✓	✓	✓	✓	✗	PD
7	Male	64	Debulking only	Temporal lobe	–	60 Gy 145 mg/day	2.0	✓	✓	✓	✓	✓	PR
8	Male	71	Biopsy	Parietal lobe	–	60 Gy 135 mg/day	26.8	✓	✓	✓	✓	✓	PD
9	Male	71	Biopsy	Frontal lobe	–	60 Gy 140 mg/day	47.6	✗	✓	✓	✓	✓	SD
10	Female	64	Debulking only	Frontal lobe	–	60 Gy 140 mg/day	13.1	✗	✓	✓	✓	✓	PR
11	Male	64	Biopsy	Frontal and parietal lobe	–	60 Gy 75 mg/day	20.9	✓	✗	✓	✗	✓	PD

[a]W2, W4, W6 and M1: PET and MRI acquisitions during RT (weeks 2, 4, and 6) and 1 month after the completion of RT (m1).
[b]PD, progressive disease; PR, partial responder; SD, stable disease, with PD and SD classified as nonresponders (NR) and PR as responder (R). ticks, acquired data; crosses, missing data; –, multifocal disease absent; +, multifocal disease present.

Table 2 Therapy response assessment using the RANO criteria

Response assessment (RANO)[a]						
Patients number	T1 Gd	T2/FLAIR signal	New lesion	Corticosteroid dose	Clinical status during treatment	Response[a]
1	$+ \geq 25\%$	Increased	–	Increased	Decline	PD
2	$- \geq 50\%$	Decreased	–	Decreased	Improved	PR
3	NA	NA	+	Increased	Decline	PD
4	NA	Increased	+	None	Decline	PD
5	$- \geq 50\%$	Stable	–	None	Stable	PR
6	$+ \geq 25\%$	Increased	–	Increased	Decline	PD
7	$- \geq 50\%$	Stable	–	None	Stable	PR
8	NA	NA	+	Stable	Stable	PD
9	$- < 50\%$ but $+ < 25\%$	Decreased	–	Stable	Improved	SD
10	$- \geq 50\%$	Stable	–	None	Stable	PR
11	$+ \geq 25\%$	Increased	–	Increased	Decline	PD

PD also occurs when a new lesion is present, making the measurement of the contrast-enhancing lesion expendable (NA, not applicable).
CR, complete responders; FLAIR, Fluid Attenuated Inversion Recovery; Gd, gadolinium; NR, nonresponders; PD, progressive disease; PR, partial responders; R, responders; RANO, Response Assessment in Neuro-Oncology; SD, stable disease.
[a]Response Assessment in Neuro-Oncology criteria were applied 6 months after the completion of RT to divide the patients into two categories: responders, including partial and complete responders, and nonresponders, including stable and progressive disease. –, new lesion absent; +, new lesion present.

imported into PMOD. PET-CT coregistration was performed automatically using the rigid matching tool (mutual information algorithm). The 95% isodose for every patient was extracted from the RT plan using the software system Eclipse (Varian Medical Systems, Palo Alto, California, USA) and was transferred onto the PET-CT fusion. Within the 95% isodose, a threshold of 40% of SUV_{max} was applied, defining MTV automatically (Fig. 1). For tumors located adjacent to the lateral ventricle, physiological uptake of ^{18}F-FCho in the choroid plexus [19] was excluded manually from the MTV. The mean and maximum SUV within the MTV were calculated (SUV_{mean} and SUV_{max}) in all repeat scans and the percentage change of these parameters between every time point was assessed.

MRI

The MR examinations were performed on a 3-Tesla Siemens Trio Tim whole-body scanner (Erlangen, Germany) using a standard 12-channel phased array head

Fig. 1

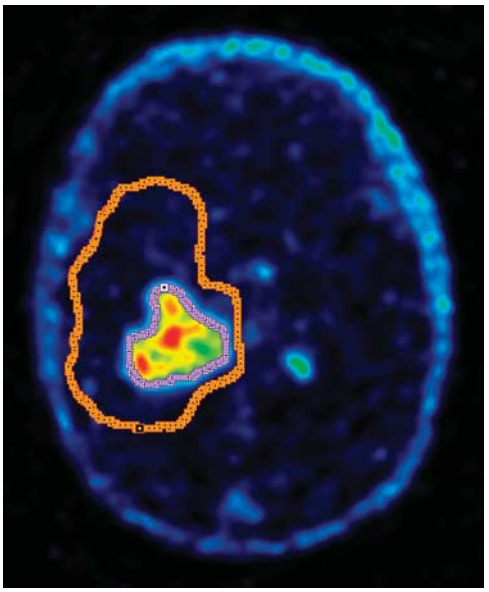

Automatic delineation of the metabolic tumor volume (MTV) on a 5 min PET image acquired 25–30 min after injection applying a threshold of 40% maximum standardized uptake value (purple) within the 95% isodose (orange) (patient 4).

coil. Structural images were acquired using a 3D T1-weighted gradient-echo sequence (MPRAGE) with isotropic voxels (176 sagittal slices, FOV read = 220 mm, voxel size $0.9 \times 0.9 \times 0.9$ mm, TR = 1550, TE = 2.39, TI = 900 ms, matrix size = 256×256, GRAPPA factor 2) and a 3D T2-weighted inversion recovery sequence (FLAIR) with isotropic voxels (176 sagittal slices, FOV read = 250 mm, voxel size $1 \times 1 \times 1$ mm, TR = 6000, TE = 421, TI = 2100 ms, matrix size = 256×238, GRAPPA factor 2). The MPRAGE sequence was repeated following the administration of gadolinium contrast.

All 3D image volumes were reconstructed in 3-mm slices in three orthogonal planes (sagittal, axial, and coronal). MRI was performed on the same day as the PET scan, or if not possible, within the same week. The contrast-enhancing tumor volume (GdTV) was calculated by a senior neuroradiologist using the IMPAX software (Agfa Healthcare, Mortsel, Belgium). The sum of products of the perpendicular diameters of each lesion was calculated. In one patient with multifocal disease, the two most voluminous lesions were measured (patient 3).

Statistical analysis

The Mann–Whitney *U*-test was used to compare SUVs, MTVs, and percentage change of all the variables between all time-points in R and NR. For all tests, an α error up to 5% ($P < 0.05$) was considered significant. Receiver operating curve (ROC) analyses were carried out to determine the cut-off value with the highest sensitivity and specificity to differentiate R from NR. The statistical tests were performed using the SPSS software (version 20; IBM, Armonk, New York, USA).

Results

Response evaluation

Applying the RANO criteria 6 months after the completion of RT, 4/11 patients (36%) were classified as R (PR) and 7/11 patients (64%) were classified as NR (SD and PD) (see also Table 2). PD was present in 6/11 patients (55%), showing a new lesion in 3/11 patients (27%) and an increase of tumor volume of at least 25% on contrast-enhanced T1-weighted MRI in 3/11 patients (27%). SD was present in 1/11 patients (see Fig. 2 for examples of PR, SD, and PD).

Semiquantitative PET analysis

Absolute SUV, MTV, and GdTV values

Absolute SUV_{mean} and SUV_{max} values were not significantly different between R and NR at any time-point (data not shown). An overview of all variables significantly different between R and NR ($P < 0.05$) is shown in Table 3. Only parameters highly significantly different between R and NR ($P \leq 0.01$) are further discussed. Only $MTV \times SUV_{mean}$ 1 month after RT was significantly higher in NR than in R ($P = 0.010$); see Fig. 3. In addition, it is worth mentioning that in three NRs, SUV_{max} decreased over time, whereas MTV increased.

Change in SUV, MTV, and GdTV values

On the basis of PET, only the change in SUV_{mean} between week 4 during RT and 1 month after RT was significantly higher in R than in NR ($P = 0.010$). For MRI, GdTV changes between week 2 and 6 ($P = 0.010$), week 4 and 6 ($P = 0.006$), and week 2 and 1 month after RT ($P = 0.010$) were significantly higher in R than in NR (Fig. 3a).

ROC analysis

A 100% sensitivity and specificity to differentiate R from NR was achieved 1 month after RT applying a cut-off value of 7.6 ccm for the PET-derived parameter $MTV \times SUV_{mean}$. Differentiation between R and NR was also achieved with 100% sensitivity and specificity by applying a decrease of at least 9% between week 4 during RT and 1 month after RT for SUV_{mean}. For GdTV, response prediction is feasible with a 100% sensitivity and specificity by applying a decrease of at least 53% between week 2 during RT and 1 month after RT, a decrease of at least 31% between week 2 and 6 during RT, and a decrease of at least 18% between weeks 4 and 6 during RT. As such, the parameter that predicts response first is MR derived, namely, GdTV.

Fig. 2

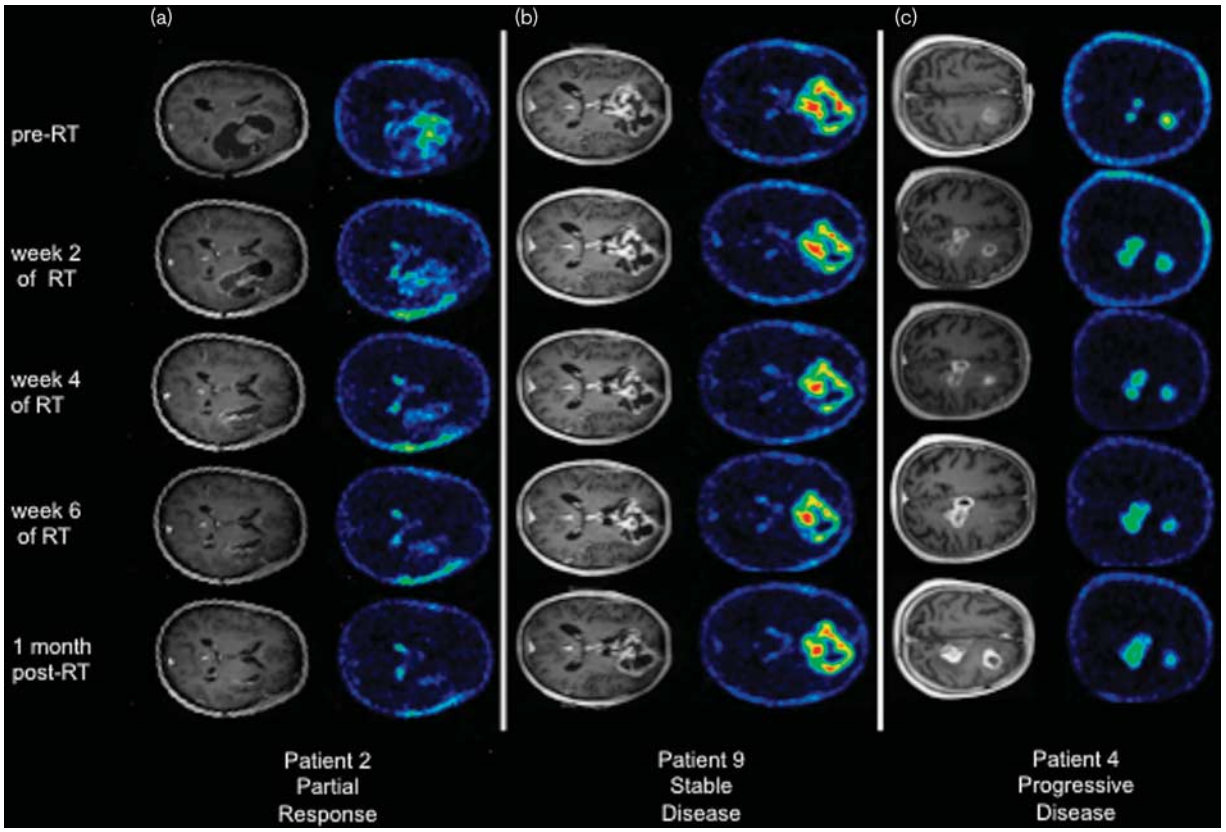

Fluorine-18 fluoromethylcholine (^{18}F-FCho) PET and contrast-enhanced T1-weighted MRI in patient 2 (a), patient 9 (b), and patient 4 (c). (a) A 47-year-old female patient diagnosed with GB in the right frontal and temporal lobe. According to the RANO criteria, the patient is categorized as a partial responder. A 60% decrease in SUV_{max} and SUV_{mean} is observed from before RT to 1 month after RT. (b) A 71-year-old male patient diagnosed with a bifrontal GB. According to the RANO criteria, the patient was categorized as having stable disease. From before RT to 1 month after RT, SUV_{max} decreased 17%, whereas SUV_{mean} remained more or less stable. (c) A 66-year-old male patient diagnosed with multifocal GB. A new lesion was visible on follow-up MRI, categorizing the patient as having progressive disease. From before RT to 1 month after RT SUV_{max} and SUV_{mean} decreased 52% and 59%, respectively, whereas MTV increased with > 300%. GB, glioblastoma; RANO, Response Assessment in Neuro-Oncology; RT, radiation therapy; SUV, standardized uptake value.

Discussion

In this study, we investigated ^{18}F-FCho PET and contrast-enhanced MRI for response assessment in 11 GB patients who were not good candidates for (maximal) surgery and received therapy according to the Stupp protocol [3]. ^{18}F-FCho PET was used because enhanced choline metabolism is a hallmark of malignancy and increased ^{18}F-FCho uptake is associated with oncogenesis and tumor progression [20–24]. ^{18}F-FCho PET has been shown to identify the boundaries of high-grade glioma because accumulation in surrounding normal brain tissue is low, making it a promising tool for diagnosis, image-guided biopsy, and therapy response assessment in primary and recurrent high-grade glioma [19,23,25,26]. In a recent review, the authors stated that ^{18}F-FCho uptake by a brain tumor reflects tumor metabolism, but that there is no strong correlation between tumor grade and choline uptake [19,23,26].

For therapy response monitoring in glioma, promising results have been reported for ^{18}F-FET PET [8,13,14]. In a study by Piroth *et al.* [13], the authors defined early treatment response in GB patients as a decrease in the maximal tumor-to-brain ratio of at least 10% between the start of RT and 7–10 days after the completion of RT. The threshold also yielded a good discriminative power to separate prognostic groups in terms of progression-free and overall survival [14]. Hutterer *et al.* [27] reported a decrease of 45% of MTV to define metabolic response in recurrent high-grade glioma patients treated with bevacizumab and irinotecan. For ^{18}F-FLT PET, more than 25% reduction in tumor SUV uptake was defined as a metabolic response in patients with recurrent malignant gliomas treated with bevacizumab and irinotecan [28]. Only a few papers have investigated ^{18}F-FCho PET for therapy response assessment in malignancies. Parashar *et al.* [29] suggested that there was a good correlation between a change in SUV_{max} of the tumor during RT and

Table 3 ROC analysis of variables significantly different between R and NR

	Variable	Time-point	*n*	Mann–Whitney *U* one tailed (*P*-value)	ROC cut-off value	ROC area under curve	Sensitivity (%)	Specificity (%)
Absolute values								
PET-based	MTV	W4	11	0.042	6.03	0.893	75	86
	MTV	W6	10	0.019	6.91	0.958	100	83
	MTV	M1	10	0.019	14.56	0.958	100	83
	MTV × SUV_{mean}	W6	10	0.019	17.66	0.958	100	83
	MTV × SUV_{mean}	**M1**	**10**	**0.010**	**7.55**	**1.000**	**100**	**100**
MR-based	GdTV	W4	11	0.042	50.22	0.893	86	100
	GdTV	W6	11	0.042	52.51	0.893	86	100
	GdTV	M1	11	0.024	30.88	0.929	100	75
Change between two time-points (%)								
PET-based	MTV	Pre-m1	8	0.071	−16.05	1.000	100	100
	MTV	W2-m1	9	0.032	0.01	0.950	100	80
	MTV × SUV_{mean}	Pre-m1	8	0.071	−23.46	1.000	100	100
	MTV × SUV_{mean}	W2-M1	9	0.016	−33.25	1.000	100	100
	SUV_{max}	W4-w6	10	0.038	7.64	0.917	100	78
	SUV_{mean}	**W4-m1**	**10**	**0.010**	**−8.53**	**1.000**	**100**	**100**
MR-based	GdTV	Pre-m1	9	0.056	−42.70	1.000	100	100
	GdTV	**W2-m1**	**10**	**0.010**	**−52.71**	**1.000**	**100**	**100**
	GdTV	Pre-w6	9	0.056	−41.60	1.000	100	100
	GdTV	W2-w4	10	0.019	−13.99	0.958	83	100
	GdTV	***W2-w6***	***10***	***0.010***	***−31.04***	***1.000***	***100***	***100***
	GdTV	***W4-w6***	***11***	***0.006***	***−17.70***	***1.000***	***100***	***100***

Bold indicates parameters that are highly significantly different ($P \leq 0.01$) between R and NR.
Italic indicates parameters that predict response first.
GdTV, contrast-enhancing tumor volume; M, month after the completion of radiation therapy; MTV, metabolic tumor volume; NR, nonresponders; Pre, pretreatment; R, responders; ROC, receiver operating curve; SUV, standardized uptake value; W, week after initiation of treatment.

Fig. 3

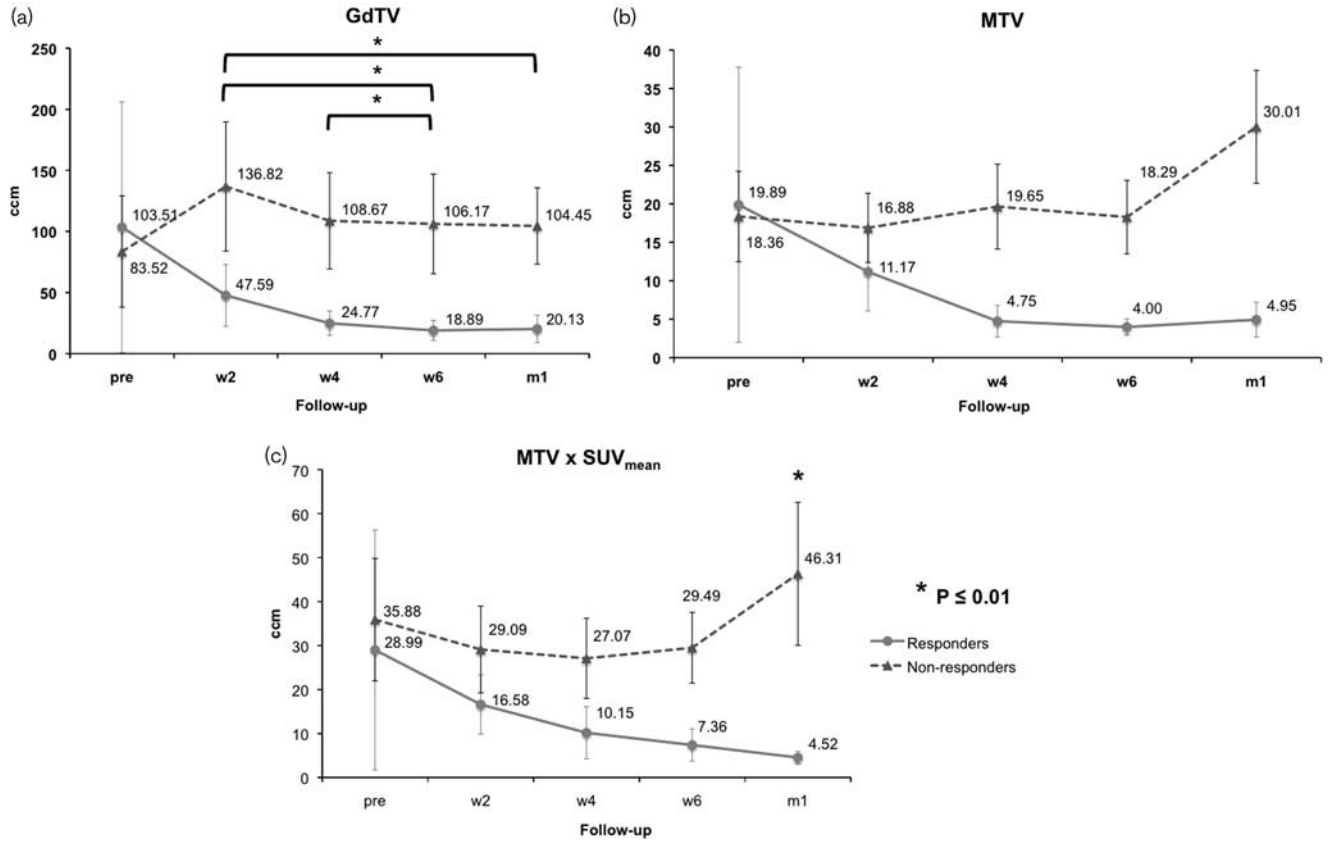

Evolution over time of the contrast-enhanced tumor volume (GdTV) (a), metabolic tumor volume (MTV) (b) and MTV × SUV_{mean} (c) in responders (R) and nonresponders (NR). Mean and standard error of the mean are presented. *Variables highly significantly different ($P \leq 0.01$) between R and NR. M, month; Pre, pretreatment; SUV, standardized uptake value; W, week.

response. However, only one patient with a malignant glioma was included in this study. In another ^{11}C-choline PET study, Li *et al.* [30] reported that a tumor-to-brain ratio up to 1.4 might predict a longer overall survival in patients with suspected recurrent glioma after treatment. It is, however, noteworthy that in the literature (early), PET response in malignant glioma is defined as decreased tracer uptake over time, but that proposed thresholds vary strongly between studies [13,14,27–30]. Importantly, different PET tracers visualize different biological processes, which probably (partly) explain the different threshold values. Also, therapy response is assessed at different time-points in different studies, which may also (partly) explain the different threshold values. In addition, cut-off values are method specific because they are affected by acquisition parameters, the choice of reconstruction algorithm, and region of interest definition [31–33]. All these factors may explain the often large differences between thresholds and underline the importance of a validation of the proposed thresholds, ideally by histology. Despite the lack of a pathological proof in our study, we studied ^{18}F-FCho uptake before, during, and after the completion of RT within the metabolically active tumor part that received at least 95% of the prescribed irradiation dose (MTV). A 40% threshold of SUV_{max} was applied because it corresponded best with the visually enhanced tracer uptake in the tumor. Moreover, it is well known that an automatic threshold technique is the best guarantee that consistent VOIs are defined on repeat scans as are acquired in our study [31,34]. Other advantages of automatic thresholding are that the method is user independent as well as independent of any changes in tumor geometry, which is of particular relevance in studies that assess therapy response because tumors may shrink as a result of effective treatments [35].

We found that absolute SUV values before RT, during RT, and 1 month after RT did not predict response. A decrease of at least 9% of SUV_{mean} between week 4 during RT and 1 month after RT differentiated R from NR with 100% sensitivity and specificity. However, changes in tracer uptake of 10–20% may be considered within the range of normal biological variability. More importantly and as mentioned above, we noted that in three NRs, absolute SUV values decreased during the course of the treatment, whereas MTV increased. This means that MTV must be taken into account. On the basis of our results, GdTV at week 6 during RT can be used for early response prediction in GB patients receiving combined RT and TMZ (Fig. 3). However, this finding warrants caution because of the possibility of pseudoprogression occurring within 12 weeks after treatment in 20–30% of GB patients [7]. On the basis of our results, an alternative is provided by the ^{18}F-FCho PET-derived parameter, $MTV \times SUV_{mean}$, which enables prediction of therapy response as early as 1 month after the completion of RT. In comparison with the results of other PET tracers in the literature and in particular ^{18}F-FET, our results indicate that ^{18}F-FCho PET is not superior to ^{18}F-FET PET, which enables prediction of response as early as 7–10 days after the completion of treatment [13, 14,36]. On the basis of our and other results in the literature, inclusion of PET in the RANO criteria might be useful for early therapy response prediction in high-grade glioma, particularly in cases diagnosed with pseudoprogression on post-treatment MRI. However, this needs to be confirmed in larger studies. It will also be of interest to investigate the clinical role of advanced MRI techniques in combination with (^{18}F-FCho) PET for early therapy response assessment in GB patients.

Conclusion

Our data indicate that ^{18}F-FCho PET and contrast-enhanced T1-weighted MRI can predict response 1 month after the completion of RT and 6 weeks after treatment initiation, respectively. Further studies investigating the role of multimodality imaging in early therapy response assessment in GB, thereby allowing patient-tailored therapy are, however, needed.

Acknowledgements

The authors would like to thank Stichting Luka Hemelaere for supporting this work.

J. Bolcaen, M. Acou, and I. Goethals, project development, data collection, data analysis, manuscript writing and editing. T. Boterberg, project development, manuscript editing. C. Vanhove, data analysis, manuscript writing and editing. F. De Vos, project development, manuscript writing and editing. C. van den Broecke, data collection, manuscript editing. R. van Holen, data analysis, manuscript editing. K. Deblaere, data collection, data analysis, manuscript writing and editing

The authors declare that the human studies have been approved by the ethics committee of the Ghent University Hospital and have therefore been carried out in accordance with the ethical standards laid down in the 1964 Declaration of Helsinki and its later amendments. We declare that all patients provided informed consent before inclusion in this study.

Conflicts of interest

There are no conflicts of interest.

References

1 Ahmed R, Oborski MJ, Hwang M, Lieberman FS, Mountz JM. Malignant gliomas: current perspectives in diagnosis, treatment, and early response assessment using advanced quantitative imaging methods. *Cancer Manag Res* 2014; **6**:149–170.
2 Anton K, Baehring JM, Mayer T. Glioblastoma multiforme: overview of current treatment and future perspectives. *Hematol Oncol Clin North Am* 2012; **26**:825–853.
3 Stupp R, Dietrich PY, Kraljevic SO, Pica A, Maillard I, Maeder P, *et al.* Promising survival for patients with newly diagnosed glioblastoma multiforme

treated with concomitant radiation plus temozolomide followed by adjuvant temozolomide. *J Clin Oncol* 2002; **20**:1375–1382.
4 Siu A, Wind JJ, Iorgulescu B, Chan TA, Yamada Y, Sherman JH. Radiation necrosis following treatment of high grade glioma:a review of the literature and current understanding. *Acta Neurochir* 2012; **154**:191–201.
5 Gorlia T, van den Bent MJ, Hegi ME, Mirimanoff RO, Weller M, Cairncross JG, *et al*. Nomograms for predicting survival of patients with newly diagnosed glioblastoma: prognostic factor analysis of EORTC and NCIC trial 26981-22981/CE.3. *Lancet Oncol* 2008; **9**:29–38.
6 Ducray F, Idbaih A, Wang XW, Cheneau C, Labussiere M, Sanson M. Predictive and prognostic factors for gliomas. *Expert Rev Anticancer Ther* 2011; **11**:781–789.
7 Wen PY, Macdonald DR, Reardon DA, Cloughesy TF, Sorenson AG, Galanis E, *et al*. Updated response assessment criteria for high-grade gliomas: response assessment in neuro-oncology working group. *J Clin Oncol* 2010; **28**:1963–1972.
8 Galldiks N, Rapp M, Stoffels G, Fink GR, Shah NJ, Coenen HH, *et al*. Response assessment of bevacizumab in patients with recurrent malignant glioma using [^{18}F]fluoroethyl-L-tyrosine PET in comparison to MRI. *Eur J Nucl Med Mol Imaging* 2013; **40**:22–33.
9 Hoekstra CJ, Paglianiti I, Hoekstra OS, Smit EF, Postmus PE, Teule GJJ, *et al*. Monitoring response to therapy in cancer using [^{18}F]-2-fluoro-2-deoxy-D-glucose and positron emission tomography – an overview of different analytical methods. *Eur J Nucl Med* 2000; **27**:731–743.
10 Dhermain FG, Hau P, Lanfermann H, Jacobs AH, van den Bent MJ. Advanced MRI and PET imaging for assessment of treatment response in patients with gliomas. *Lancet Neurol* 2010; **9**:906–920.
11 Mertens K, Acou M, van Hauwe J, De Ruyck I, van den Broecke C, Kalala JP, *et al*. Validation of ^{18}F-FDG PET at conventional and delayed intervals for the discrimination of high-grade from low-grade gliomas. *Clin Nucl Med* 2013; **38**:495–500.
12 Spence AM, Muzi M, Mankoff DA, O'Sullivan SF, Link JM, Lewellen TK, *et al*. ^{18}F-FDG PET of gliomas at delayed intervals: improved distinction between tumor and normal gray matter. *J Nucl Med* 2004; **45**:1653–1659.
13 Piroth MD, Pinkawa M, Holy R, Klotz J, Nussen S, Stoffels G, *et al*. Prognostic value of early [^{18}F]fluoroethyltyrosine positron emission tomography after radiochemotherapy in glioblastoma multiforme. *Int J Radiat Oncol Biol Phys* 2011; **80**:176–184.
14 Galldiks N, Langen KJ, Holy R, Pinkawa M, Stoffels G, Nolte KW, *et al*. Assessment of treatment response in patients with glioblastoma using O-(2-^{18}F-fluoroethyl)-L-tyrosine PET in comparison to MRI. *J Nucl Med* 2012; **53**:1048–1057.
15 Wyss M, Hofer S, Bruehlmeier M, Hefti M, Uhlmann C, Bärtschi E, *et al*. Early metabolic responses in temozolomide treated low-grade glioma patients. *J Neurooncol* 2009; **95**:87–93.
16 Schwarzenberg J, Czernin J, Cloughesy TF, Ellingson BM, Pope WB, Grogan T, *et al*. Treatment response evaluation using ^{18}F-FDOPA PET in patients with recurrent malignant glioma on bevacizumab therapy. *Clin Cancer Res* 2014; **20**:3550–3559.
17 Slaets D, De Bruyne S, Dumolyn C, Moerman L, Mertens K, De Vos F. Reduced dimethylaminoethanol in [(^{18})F] fluoromethylcholine: an important step towards enhanced tumour visualization. *Eur J Nucl Med Mol Imaging* 2010; **37**:2136–2145.
18 Cheebsumon P, Yaqub M, van Velden FHP, Hoekstra OS, Lammerstma AA, Boellaard R. Impact of [(^{18})F]FDG PET imaging parameters on automatic tumour delineation: need for improved tumour delineation methodology. *Eur J Nucl Med Mol Imaging* 2011; **38**:2136–2144.
19 Mertens K, Ham H, Deblaere K, Kalala JP, van den Broecke C, Slaets D, *et al*. Distribution patterns of ^{18}F-labelled fluoromethylcholine in normal structures and tumors of the head. A PET/MRI evaluation. *Clin Nucl Med* 2012; **37**: e196–e203.
20 Kwee SA, Coel MN, Lim J, JP K. Prostate cancer localization with 18 fluorine fluorocholine positron emission tomography. *J Urol* 2005; **173**:252–255.
21 Kwee SA, Wei H, Sesterhenn I, Yun D, Coel MN. Localization of primary prostate cancer with dual-phase ^{18}F-fluorocholine PET. *J Nucl Med* 2006; **47**:262–269.
22 Husarik DB, Miralbell R, Dubs M, John H, Giger OT, Gelet A. Evaluation of [^{18}F]-choline PET{2F}CT for staging and restaging of prostate cancer. *Eur J Nucl Med Mol Imaging* 2008; **35**:253–263.
23 Mertens K, Slaets D, Lambert B, Acou M, De Vos F, Goethals I. PET with (^{18}) F-labelled choline-based tracers for tumour imaging: a review of the literature. *Eur J Nucl Med Mol Imaging* 2010; **37**:2188–2193.
24 Talbot JN, Gutman F, Fartoux L, Grange JD, Ganne N, Kerrou K, *et al*. PET/CT in patients with hepatocellular carcinoma using [^{18}F]fluorocholine: preliminary comparison with [^{18}F]FDG PET/CT. *Eur J Nucl Med Mol Imaging* 2006; **33**:1285–1289.
25 Kwee SA, Ko JP, Jiang CS, Watters MR, Coel MN. Solitary brain lesions enhancing at MR imaging: evaluation with fluorine 18-fluorocholine PET. *Radiology* 2007; **244**:557–565.
26 Calabria FF, Barbarisi M, Gangemi V, Grillea G, Cascini GL. Molecular imaging of brain tumors with radiolabeled choline PET. *Neurosurg Rev* 2016. [Epub ahead of print].
27 Hutterer M, Nowosielski M, Putzer D, Waitz D, Tinkhauser G, Kostron H, *et al*. O-(2-^{18}F-fluoroethyl)-L-tyrosine PET predicts failure of antiangiogenic treatment in patients with recurrent high-grade glioma. *J Nucl Med* 2011; **52**:856–864.
28 Chen W, Delaloye S, Silvermann DHS, Geist C, Czemin J, Sayre J, *et al*. Predicting treatment response of malignant gliomas to bevacizumab and irinotecan by imaging proliferation with (^{18}F) fluorothymidine positron emission tomography: a pilot study. *J Clin Oncol* 2007; **25**:4714–4721.
29 Parashar B, Wernicke AG, Rice S, Osborne J, Singh P, Nori D, *et al*. Early assesment of radiation response using a novel functional imaging modality-[^{18}F]fluorocholine PET (FCH-PET): a pilot study. *Discov Med* 2012; **14**:13–20.
30 Li W, Ma L, Wang X, Sun J, Wang S, Hu X. ^{11}C-choline PET/CT tumor recurrence detection and survival prediction in post-treatment patients with high-grade gliomas. *Tumor Biol* 2014; **35**:12353–12360.
31 Lammerstma AA, Hoekstra CJ, Giaccone G, Hoekstra OS. How should we analyse FDG PET studies for monitoring tumour response? *Eur J Nucl Med Mol Imaging* 2006; **33**:S16–S21.
32 Boellaard R. Standards for PET image acquisition and quantitative data analysis. *J Nucl Med* 2009; **50**:11S–20S.
33 Cheebsumon P, van Velden FHP, Yaqub M, Frings V, de Langen AJ, Hoekstra OS, *et al*. Effects of image characteristics on performance of tumor delineation methods: a test-retest assessment. *J Nucl Med* 2011; **52**:1550–1558.
34 Jeraj R, Bradshaw T, Simoncic U. Molecular imaging to plan radiotherapy and evaluate its efficacy. *J Nucl Med* 2015; **56**:1752–1765.
35 Krak NC, Boellaad R, Hoekstra OS, Twisk JWR, Hoekstra CJ, Lammerstma AA. Effects of ROI definition and reconstruction method on quantitative outcome and applicability in a response monitoring trial. *Eur J Nucl Med Mol Imaging* 2005; **32**:294–301.
36 Roelcke U, Bruehlmeier M, Hefti M, Hundsberger T, Nitzsche EU. F-18 choline PET does not detect increased metabolism in F-18 fluoroethyltyrosine-negative low-grade gliomas. *Clin Nucl Med* 2012; **37**: e1–e3.